Cell Reports
Medicine

Report

Efficacy of glucagon-like peptide-1 and estrogen dual agonist in pancreatic islets protection and pre-clinical models of insulin-deficient diabetes

Graphical abstract

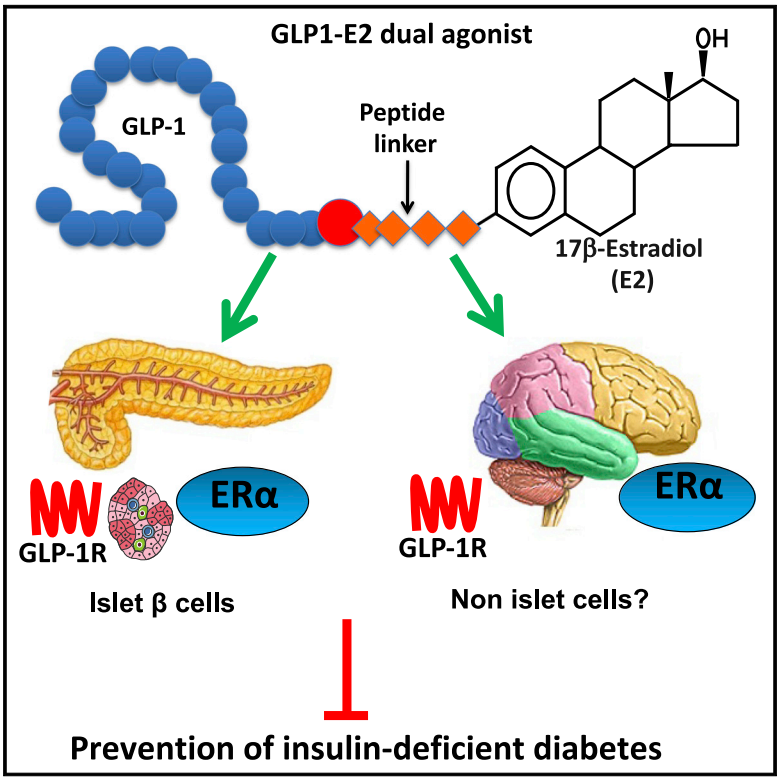

Highlights

- GLP1-E2 enhances GLP-1-mediated protection of insulin-deficient diabetes in mice
- GLP1-E2 activates ERα following GLP-1R internalization and lysosomal acidification
- GLP1-E2 amplifies antiapoptotic pathways activated by GLP-1 in human β cells
- GLP1-E2 antidiabetic actions involve GLP-1R-expressing cells outside the islets

Authors

Taylor Fuselier, Paula Mota de Sa, M.M. Fahd Qadir, ..., Sarah H. Lindsey, Richard D. Dimarchi, Franck Mauvais-Jarvis

Correspondence

fmauvais@tulane.edu

In brief

Fuselier et al. report that a glucagon-like peptide-1 and estrogen dual agonist (GLP1-E2) provides superior protection from insulin-deficient diabetes in mice compared to GLP-1 and E2 monoagonists, via targeted delivery to GLP-1 receptor (GLP-1R) and estrogen receptor-α (ERα) in β cells, and non-islet cells co-expressing GLP-1R and ERα.

Fuselier et al., 2022, Cell Reports Medicine *3*, 100598
April 19, 2022
https://doi.org/10.1016/j.xcrm.2022.100598

CellPress

Cell Reports Medicine

CellPress
OPEN ACCESS

Report

Efficacy of glucagon-like peptide-1 and estrogen dual agonist in pancreatic islets protection and pre-clinical models of insulin-deficient diabetes

Taylor Fuselier,[1,8] Paula Mota de Sa,[1,2,3,8] M.M. Fahd Qadir,[1,2,3,8] Beibei Xu,[1] Camille Allard,[1] Mathew M. Meyers,[4] Joseph P. Tiano,[4] Bin S. Yang,[5] Vasily Gelfanov,[5] Sarah H. Lindsey,[2,6] Richard D. Dimarchi,[7] and Franck Mauvais-Jarvis[1,2,3,9,*]

[1]Deming Department of Medicine, Section of Endocrinology and Metabolism, Tulane University School of Medicine, 1430 Tulane Avenue, New Orleans, LA 70112, USA
[2]Tulane Center of Excellence in Sex-Based Biology & Medicine, New Orleans, LA 70112, USA
[3]Southeast Louisiana Veterans Healthcare System Medical Center, New Orleans, LA 70119, USA
[4]Department of Medicine, Feinberg School of Medicine, Northwestern University, Chicago, IL 60611, USA
[5]Novo Nordisk Research Center Indianapolis, Indianapolis, IN 46241, USA
[6]Department of Pharmacology, Tulane University School of Medicine, New Orleans, LA 70112, USA
[7]Department of Chemistry, Indiana University, Bloomington, IN 47405, USA
[8]These authors contributed equally
[9]Lead contact
*Correspondence: fmauvais@tulane.edu
https://doi.org/10.1016/j.xcrm.2022.100598

SUMMARY

We study the efficacy of a glucagon-like peptide-1 (GLP-1) and estrogen dual agonist (GLP1-E2) in pancreatic islet protection. GLP1-E2 provides superior protection from insulin-deficient diabetes induced by multiple low-dose streptozotocin (MLD-STZ-diabetes) and by the Akita mutation in mice than a GLP-1 monoagonist. GLP1-E2 does not protect from MLD-STZ-diabetes in estrogen receptor-α (ERα)-deficient mice and fails to prevent diabetes in Akita mice following GLP-1 receptor (GLP-1R) antagonism, demonstrating the requirement of GLP-1R and ERα for GLP1-E2 antidiabetic actions. In the MIN6 β cell model, GLP1-E2 activates estrogen action following clathrin-dependent, GLP-1R-mediated internalization and lysosomal acidification. In cultured human islet, proteomic bioinformatic analysis reveals that GLP1-E2 amplifies the antiapoptotic pathways activated by monoagonists. However, in cultured mouse islets, GLP1-E2 provides antiapoptotic protection similar to monoagonists. Thus, GLP1-E2 promotes GLP-1 and E2 antiapoptotic signals in cultured islets, but *in vivo*, additional GLP1-E2 actions in non-islet cells expressing GLP-1R are instrumental to prevent diabetes.

INTRODUCTION

Protecting the functional mass of insulin-producing β cells is a major therapeutic challenge in patients with type 1 (T1D) and type 2 diabetes (T2D). In rodent models, estrogenic compounds protect β cells survival and function in the face of multiple diabetic insults.[1–10] Estrogens also protect human islets from metabolic stresses in culture and *in vivo*.[5,6,10] Randomized placebo-controlled trials have reported a significant reduction in the incidence of diabetes in women assigned to menopausal estrogen therapy, providing further evidence for the antidiabetic action of estrogens in women. One of the challenges of general estrogen therapy in diabetes, however, lies in the adverse effects of systemic estrogen action.[11]

We previously explored the preferential targeting of estradiol (E2) to the islet β cells using glucagon-like-peptide-1 (GLP-1)-based fusion peptides. By marrying the pharmacologies of GLP-1 and E2, we envisioned a synergism on islet β cells that express both GLP-1 receptors (GLP-1R) and estrogen receptors (ERs) while improving the therapeutic index of estrogens. Conjugates with GLP-1 made resistant to dipeptidyl peptidase-4 (DPP-4) and stably linked E2 were synthesized (GLP1-E2).[12] Such GLP1-E2 conjugates avoid E2 release in circulation, lack adverse effects of estrogen action in breast and uterus, and maximize E2 release in GLP-1R-expressing target cells.[12,13] In mice with diet-induced metabolic syndrome, GLP1-E2 conjugates exhibited synergistic anti-obesity properties above those of single agonists (GLP-1 or E2). In the New Zealand obese (NZO) mouse, a model of type 2 diabetes (T2D), in contrast to GLP-1, GLP1-E2 suppressed food intake and weight gain, thus preventing T2D.[14] The GLP1-E2 dual agonist also provided additional efficacy relative to GLP-1 monoagonist on insulin sensitivity and glucose homeostasis in wild-type male mice.[13] Here, we investigated unexplored aspects of the GLP1-E2 dual agonist in islet biology. First, does the GLP1-E2 dual agonist provide additional benefits relative to either GLP-1 or E2 monoagonists in protecting islet survival at the onset of insulin-deficient diabetes in animal models? Second, what are the mechanisms of

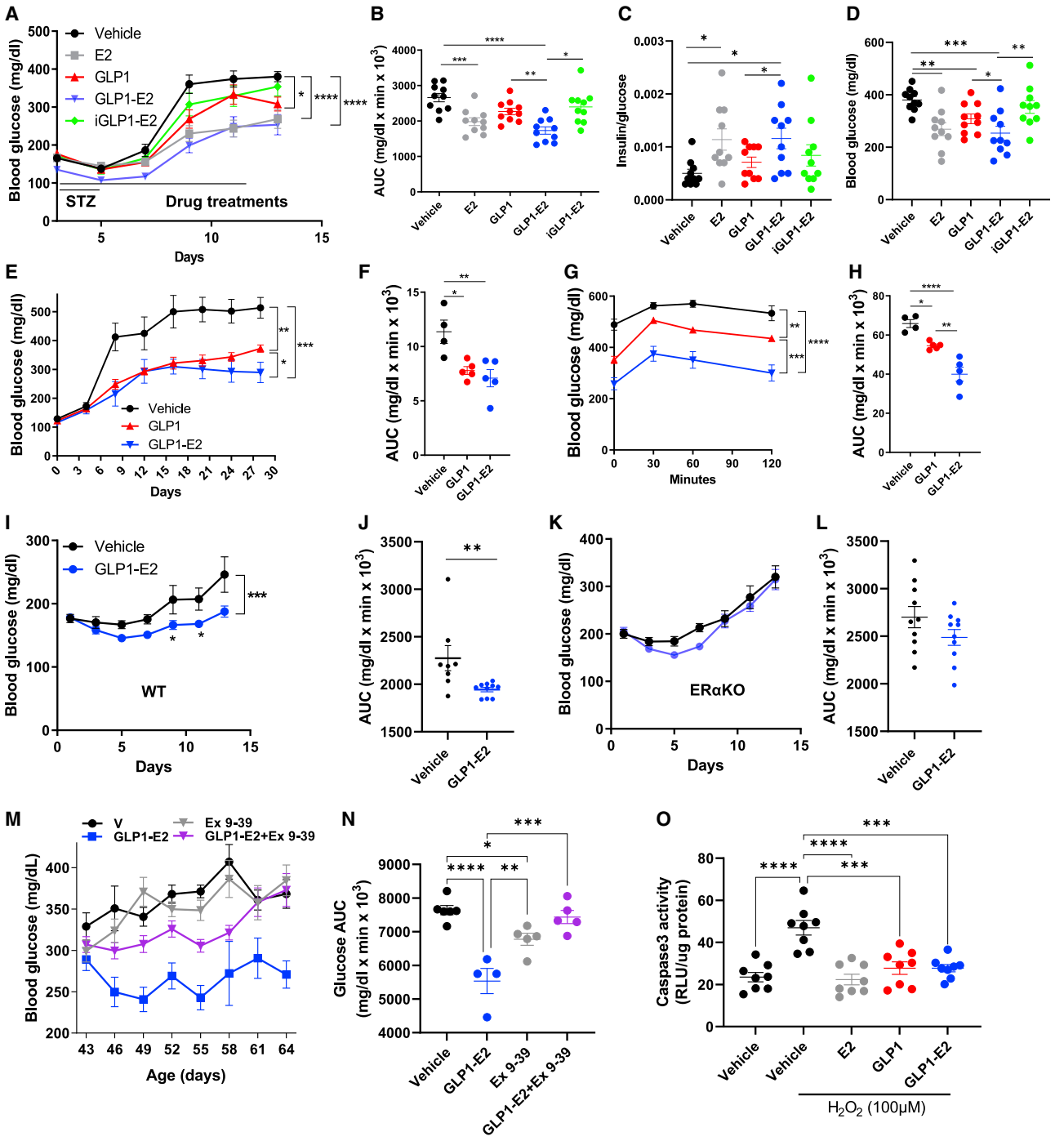

Figure 1. GLP1-E2 partially protects against insulin-deficient diabetes via GLP-1R and ERα

(A) Effects of GLP1-E2 conjugates (120 μg/kg/day) on MLD-STZ-induced diabetes in male C57BL6 mice at the indicated times (n = 10 per condition).

(B) Blood glucose area under the curve (AUC) from (A).

(C) Insulin/glucose ratio at day 13 from (A).

(D) Blood glucose at day 13 from (A).

(E) Effect of GLP1-E2 conjugates (120 μg/kg/day) on blood glucose in male Akita mice at the indicated times (n = 4–5 per condition) and (F) associated glucose AUC.

(G) IP-GTT and (H) corresponding glucose AUC in Akita mice from (E) at day 27.

(I) Effects of GLP1-E2 on MLD-STZ-induced diabetes in female WT mice at the indicated times (n = 8–10 per condition) with (J) corresponding glucose AUC.

(legend continued on next page)

GLP1-E2 fusion peptide entry in β cells and release of E2 for subsequent ER activation? Finally, does GLP1-E2 dual agonist recapitulate signaling pathways activated by the monoagonists (GLP-1 and E2) in cultured human islets?

RESULTS

GLP1-E2 partially protects against insulin-deficient diabetes via GLP-1R and ERα

E2 prevents insulin-deficient diabetes induced by a single high dose of streptozotocin (STZ) in male and female mice.[4] Here, we tested the efficacy of GLP1-E2 conjugates (120 μg/kg/day) in preventing β cell destruction in comparison to E2 in a male mouse model of multiple low-dose (MLD) injections of STZ. The MLD-STZ induces immune-mediated β cell destruction via cytotoxic activity of macrophages, T cells, and natural killer lymphocytes[15–19] and represents a good model to test the ability of GLP1-E2 peptides to prevent inflammatory islet destruction. GLP1-E2 has proven successful in decreasing blood glucose after the onset of MLD-STZ-induced diabetes.[20] To test the ability of compounds to prevent β cell destruction, we administered all agonists starting before the first injection of STZ and for a duration of 12 days, to cover the phase of islet inflammation (7 days after the last STZ injection). Mice treated with GLP-1 or an inactive GLP-1 covalently fused to E2 (iGLP1-E2, used as a control[12]) showed minor or no significant prevention of MLD-STZ-induced diabetes, respectively (Figures 1A–1D). In contrast, treatment with E2 and GLP1-E2 significantly prevented the development of β cell failure as evidenced by a decrease in hyperglycemia and maintenance of the index of β cell function (insulin/glucose) compared to other treatments (Figures 1A–1D). Similar results were obtained with GLP1-E2 at the higher dose of 400 μg/kg (Figures S1B–S1D). The GLP-1 tolerability in humans is a limitation for translation of high potency agonist-based strategies, as GLP-1R agonists produce gastrointestinal side effects at high doses;[21–23] the dose used in mice is several hundred times higher than humans can tolerate. Therefore, we tested the efficacy of GLP1-E2 conjugates in preventing MLD-STZ at a dose ten times lower (12 μg/kg). Under these conditions, GLP1-E2 still produced a significant prevention of MLD-STZ-induced diabetes (Figures S1E–S1G). The body weights of mice exposed to MLD-STZ are shown on Figure S1 and show no changes between GLP-1 conjugates. We next tested the ability of GLP1-E2 to delay spontaneous insulin-deficient diabetes in the male Akita mouse, in which mutant and misfolded proinsulin triggers early ER stress and irreparable unfolded protein response leading to β cell destruction.[24] Estrogens prevent β cell destruction by activating endoplasmic reticulum-associated protein degradation in male and female Akita mice.[10] In young male Akita mice, and similar to MLD-STZ, GLP1-E2 (120 μg/kg) delayed the development of diabetes to an extent superior to that of GLP-1 alone (Figures 1E–1H). Further, GLP1-E2 also delayed the development of diabetes at a dose of 12 μg/kg (Figures S1H and S1I).

To investigate the role of the GLP-1R in the ability of GLP1-E2 to delay diabetes, we treated male Akita mice with GLP1-E2 (12 μg/kg) in the presence or absence of exendin (9–39), a GLP-1R antagonist.[25] Under these conditions, and consistent with the importance of GLP-1Rs in mediating GLP1-E2 effects *in vivo*, the ability of GLP1-E2 to attenuate hyperglycemia was abolished by exendin (9–39) (Figures 1M and 1N). We tested the efficacy of GLP1-E2 in preventing MLD-STZ in wild-type and littermate ERα-deficient mice (ERαKO). Consistent with the importance of ERα, the ability of GLP1-E2 to attenuate MLD-STZ diabetes in WT mice was abolished in ERαKO mice (Figures 1I–1L). Note that GLP1-E2 produced no feminizing effects in male mice as assessed by serum luteinizing hormone, testosterone, and E2 concentrations, as well as prostate weight (a marker of androgenicity) (Figures S2A and S2B), and it showed no significant effect on blood pressure and heart rate (Figure S2C). In a parallel experiment, we compared GLP1-E2 to GLP-1 and E2 in preventing oxidative stress-induced apoptosis in cultured male wild-type mouse islets. Pretreatment with GLP-1, E2, and GLP1-E2 prevented H_2O_2-induced islet cell apoptosis as measured by caspase 3 activity to a similar extent, suggesting that these compounds harbor similar pro-survival effects (Figure 1O).

GLP1-E2 is internalized via clathrin-mediated endocytosis and GLP-1R

The agonist activity of GLP-1 promotes ligand-activated, clathrin-mediated endocytosis of GLP-1R at target β cells.[26,27] To assess the effect of GLP1-E2 on receptor-dependent internalization, we synthesized rhodamine-labeled GLP1-E2 conjugates (Figure S3A). The *in vitro* potency of these compounds was not altered by rhodamine (Figure S3B). We used live-cell confocal microscopy to quantify rates of internalization of rhodamine-labeled E2 conjugated peptides (GLP1-E2-Rho or iGLP1-E2-Rho) in real time. We used the rhodamine signal occurring inside the cells over a 15-min time course as a readout. We quantified internalization of GLP1-E2 compared to iGLP1-E2 in the MIN6 insulin-secreting mouse cell line in the presence or absence of Pitstop-2, an inhibitor of clathrin-mediated endocytosis.[28] Under these conditions, GLP1-E2, but not iGLP1-E2, was internalized, and this was not observed following pre-incubation with Pitstop-2 (compare Figures 2A, 2C, and S3C with Figures 2B, 2C, and S3C), suggesting that GLP1-E2 enters the cells via clathrin-mediated endocytosis.

To further examine GLP1-E2 internalization and mode of action, we developed an estrogen-responsive MIN6 cell line stably transduced with a green fluorescent protein (GFP) under the control of an estrogen response element (ERE-GFP). This model allows semi-quantitative detection of E2 delivery and action by conjugated peptides. In this model, as expected, exposure to E2 for 24 h increased the percentage of ERE-activated MIN6 cells by 4.7-fold, and this was reversed by pretreatment with the ER antagonist fulvestrant (Figures 2D and 2E). Treatment

(K) MLD-STZ-induced diabetes in littermate ERαKO mice at the indicated times (n = 10 per condition) with (L) corresponding glucose AUC.
(M) Effect of GLP1-E2, exendin 9-39 and both on blood glucose in male Akita mice at the indicated age (n = 4–6 per condition) and (N) associated glucose AUC.
(O) Caspase 3/7 activity measured in cultured WT mouse islets treated with E2 and GLP1-E2 conjugates (10^{-8} M) for 24 h, followed by exposure to H_2O_2 (100 μM) for the last 5 h. Values represent the mean ± SEM from n = 2 experiments done with eight islet replicates *p < 0.05, **p < 0.01, ***p < 0.001.

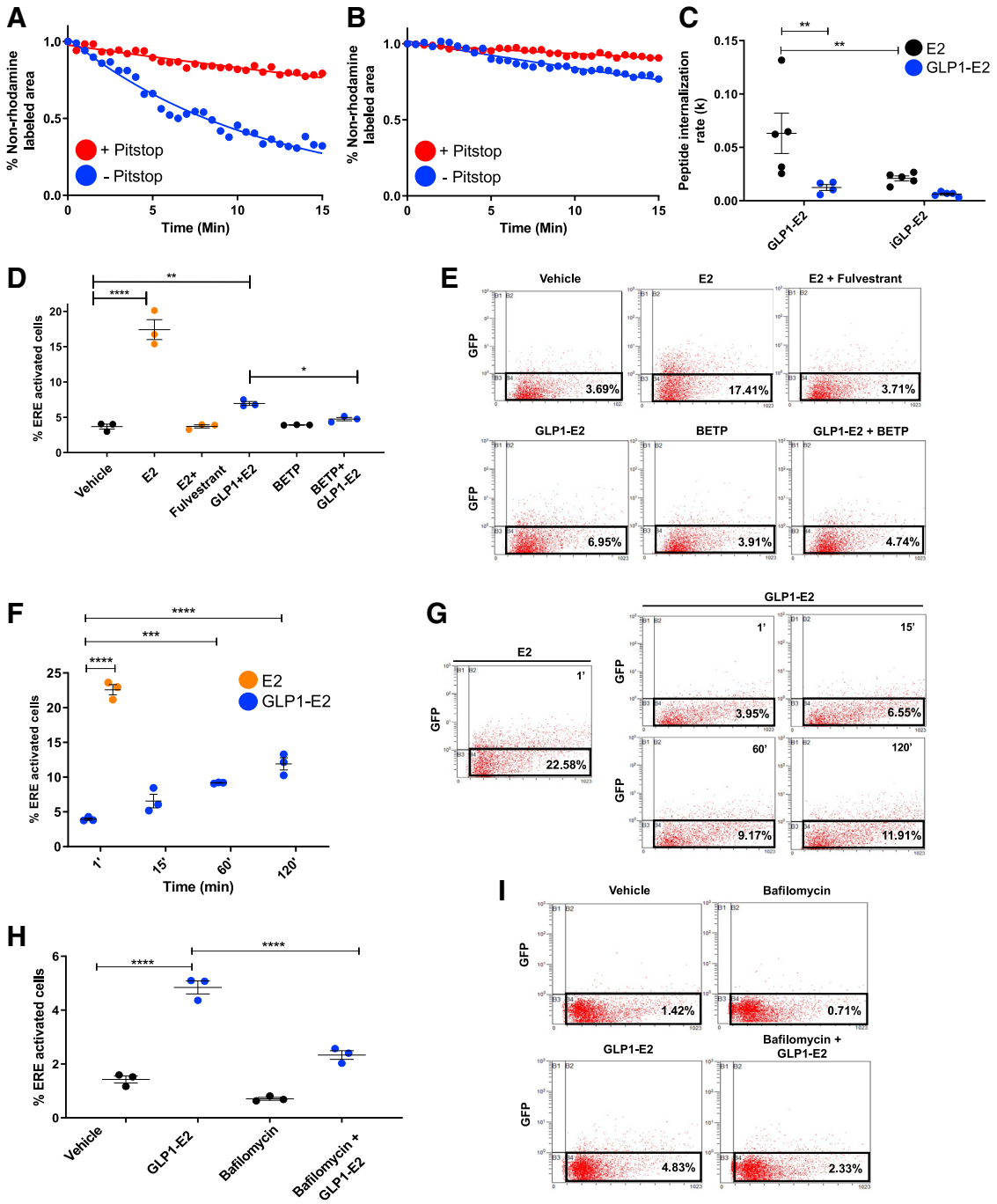

Figure 2. GLP1-E2 activates E2 action following clathrin-dependent, GLP-1R internalization and lysosomal acidification

Internalization of rhodamine-labeled (A) GLP1-E2 and (B) iGLP1-E2 signals (loss in percent object area) over time in live MIN6 cells treated with GLP-1 compounds in the presence or absence of Pitstop-2 (25μM).

(C) Rates of peptide internalization calculated from one-phase decay line fitting of (A) and (B).

(D) MIN6 cells transduced with a lentivirus delivering an ERE-GFP reporter were treated overnight with E2 (10^{-8} M), fulvestrant (10^{-6} M), GLP1-E2 (10^{-8} M), and BETP (10^{-7} M). The percentage of GFP ERE-GFP-positive MIN6 cells was quantified by flow cytometry.

(E) Representative pictures of flow cytometry with average positive percent cells from (D).

(F) ERE-GFP MIN6 cells were incubated with either 10 nM E2 for 1 min or 100 nM GLP1-E2 for 1, 15, 60, and 120 min. The percentage of GFP-positive ERE-GFP MIN6 cells was quantified by flow cytometry.

(legend continued on next page)

with GLP1-E2 also increased the percentage of ERE-activated MIN6 cells by 1.9-fold, demonstrating that once GLP1-E2 is internalized, E2 is released from the GLP1 peptide to activate nuclear ERs (Figures 2D and 2E). The proposed mechanism of E2 release from the GLP-1 peptide first involves peptide binding to the GLP-1R followed by peptide/receptor internalization in an endosomal compartment to await further intracellular processing.[12] To test whether the mechanism of cellular entry of GLP1-E2 peptides involves GLP-1R internalization, we treated ERE-GFP MIN6 cells with GLP1-E2 in the presence of BETP (also known as compound B), a selective GLP-1R allosteric modulator and agonist that impairs GLP-1R internalization.[29,30] Under these conditions, BETP abolished the ability of GLP1-E2 to activate ERE-GFP MIN6 cells (Figures 2D and 2E), consistent with GLP1-E2 being internalized via GLP-1R followed by activation of ER signaling. Additional evidence of the importance of the GLP1-R in mediating GLP1-E2 action in islets was provided by an experiment of glucose-stimulated insulin secretion in static incubation. Under these conditions, the insulinotropic effect of GLP1-E2, but not iGLP1-E2, was observed in WT islets. However, the insulinotropic effect of GLP1-E2 was not observed in islets lacking GLP-1R selectively in β cells (Figure S4A).

GLP1-E2 activates E2 action following lysosomal acidification

Incubation with E2 alone for 1 min resulted in a 6.1-fold increase in ERE-activated MIN6 cells, indicative of spontaneous and rapid steroid entry into cells (compare E2 in Figures 2F and 2G with E2 in Figures 2D and 2E). In contrast, a progressive increase in incubation time with GLP1-E2 was necessary to produce a gradual increase in the percentage of ERE-activated MIN6 cells that reached only 2-fold the level of basal after 2 h incubation (Figures 2F and 2G). Exposure to GLP1-E2 at a higher concentration (100 nM) for 24 h was necessary to increase the percentage of ERE-activated MIN6 cells by 5-fold (Figure S4B). We attribute the progressive increase in ERE-activated MIN6 cells to GLP1-E2 intracellular transport in endosomes and processing by lysosomal degradation of the peptide linker to release E2. To address this, we incubated ERE-GFP MIN6 cells with bafilomycin A1, a vacuolar H^+-ATPase inhibitor that prevents lysosomal acidification.[31] Under these conditions, pretreatment with bafilomycin blocked the ability of GLP1-E2 to activate ERE-GFP MIN6 cells, suggesting that lysosomal acidification is necessary for GLP1-E2 action (Figures 2H and 2I). Together, these data suggest that GLP1-E2 enters β cells through clathrin-dependent, GLP1R-mediated internalization, followed by E2 release after intracellular lysosomal acidification and peptide degradation, allowing free E2 to activate nuclear ERE.

GLP1-E2 recapitulates signaling pathways activated by GLP-1 and E2 in human islets

We next compared the ability of GLP1-E2 with that of GLP-1 or E2 monoagonists to activate intracellular signaling networks by functional proteomics using a reverse phase protein array (RPPA) (Figure 3). As most of our data were generated in male mice and islets as well as male MIN6 cells, we used cultured islets from male human donors. We analyzed the phosphoproteomics using Ingenuity Pathway Analysis (IPA) to highlight major activated or inhibited biological functions or disease pathways. Focusing on GLP1, E2, or GLP1-E2 stimulation at 5 min, the most represented biological function was "Cell Death & Survival" (Figure S5). For the three compounds, annotations exhibiting the highest p value and predicting pathway activation (Z score > 2) were related to cell viability and survival, whereas pathways predicting inhibition (Z score < −2) were related to cell death, apoptosis, or necrosis (Figure 3A).

Individual changes in phosphoproteins are shown in Figure 3B. Compared to GLP-1 or GLP1-E2, E2-treated islets exhibited a heightened level of phosphoproteins and related total proteins at 5 and 30 min, followed by a decreased in phosphoproteins at 18 h (Figure 3B). Overall, islets treated with the GLP1-E2 dual agonist exhibited a pattern of phosphoproteins and related total proteins combining signals from the two monoagonists (Figure 3B). This suggests that GLP1-E2 dual agonism efficiently integrates signals from GLP-1 and E2 monoagonists.

To gain additional mechanistic insights on pathways modulated by the three compounds, we performed a gene ontology (GO) enrichment analysis of proteins expression following 18 h of treatment (Figure 4A). We focused on the "Biological Process" domain and considered the main annotations (pathways) that were up- or downregulated by the three compounds with an adjusted p value < 0.01. GLP-1 upregulated few proteins enriched in pathways involved in response to cytokines and glycolysis and downregulated multiple proteins enriched in pathways involved in apoptosis, cytokine and oxidative stress-related inflammation, protein phosphorylation, Akt/PI3-kinase, and cell cycle (Figure 4A). Similarly, E2 upregulated few proteins enriched in pathways involved in proliferation and response to estrogen but downregulated multiple proteins enriched in pathways involved in apoptosis and inflammation, protein phosphorylation, transcription, and Akt/PI3-kinase (Figure 4A). Notably, compared to GLP-1 and E2, GLP1-E2 upregulated more proteins enriched in pathways involved in prevention of apoptosis (including Akt and PI3-kinase), response to cytokines and oxidative stress, angiogenesis, proliferation, glycolysis, and response to insulin and estrogen. However, compared to GLP-1 and E2, GLP1-E2 downregulated fewer proteins enriched in apoptosis and necrosis pathways (Figure 4A).

Like the individual phosphoproteins described earlier (Figure 3B), E2-treated islets exhibited a heightened protein expression at 5 and 30 min, followed by a decreased protein expression level at 18 h compared to GLP-1- and GLP1-E2-treated islets (Figure 4B). Multiple proteins exhibited a similar expression pattern among E2- and GLP1-E2-treated islets, where GLP1-E2 seemed to delay or prolong protein expression up to 18 h compared to E2 (Figure 4B), which is consistent with the time

(G) Representative pictures of flow cytometry with average positive percent cells from (H).
(H) ERE-GFP MIN6 cells were treated overnight with GLP1-E2 in the presence or absence of Bafilomycin A1 (10 nM).
(I) Representative pictures of flow cytometry with average positive percent cells from (H). Data show scatterplot with mean ± SEM from n ≥ 4 experiments done in triplicates, *p < 0.05, **p < 0.01, ***p < 0.001.

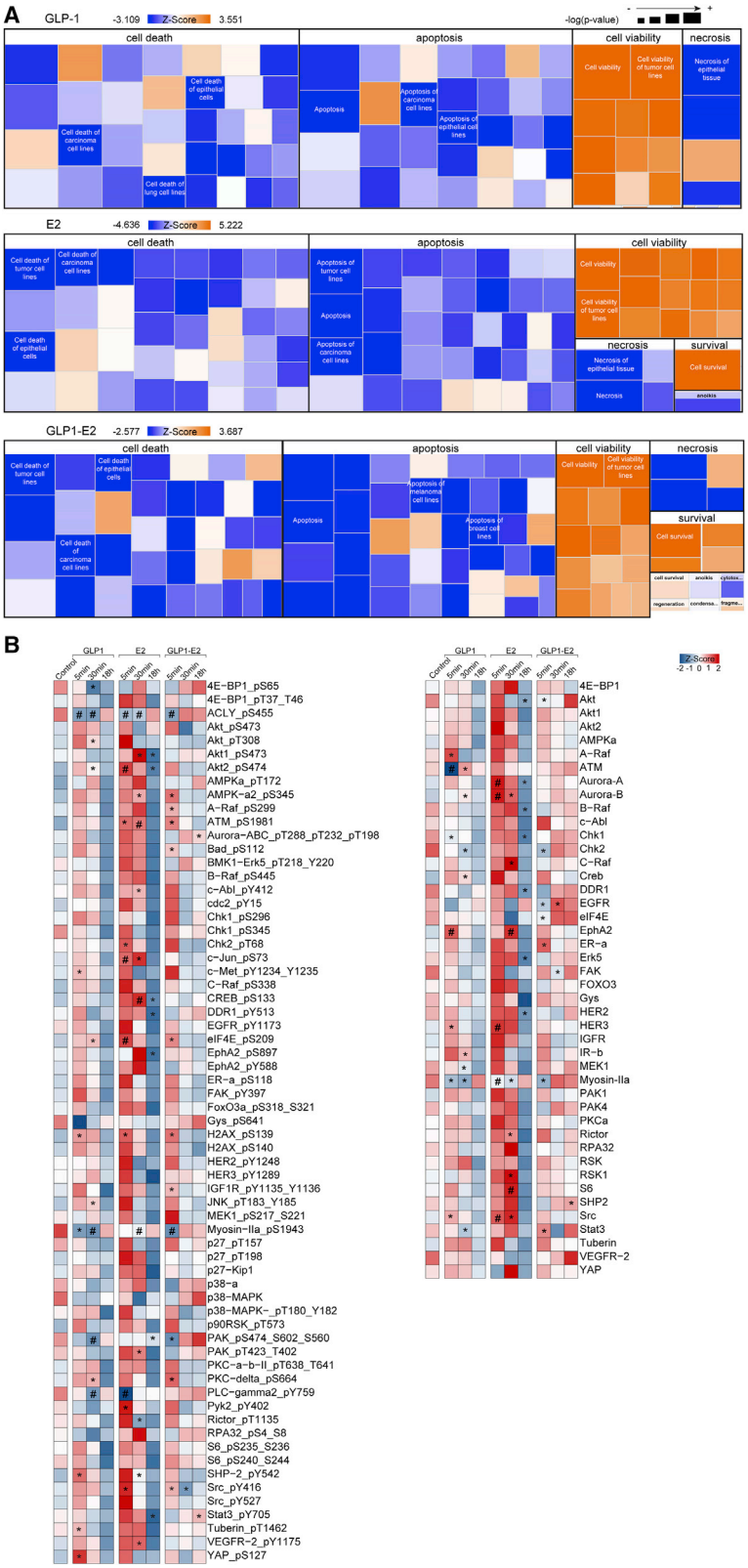

Figure 3. Effects of GLP-1, E2, and GLP1-E2 on phosphoproteins in human islets

Human islets (N = 3 donors) were treated with GLP-1, E2, or GLP1-E2 for 5 min, 30 min, and 18 h, compared to control untreated islets, and studied by RPPA.

(A) Bioinformatic analysis of phosphoproteins pathways at 5 min into the treatment using Integrated Pathway Analysis. The heatmap shows square size as a quantitative measure of –log(p value) and color intensity as a quantitative measure of *Z* score. Predicted activated or inhibited pathways are labeled in white font.

(B) Heatmap of individual phosphoproteins. Normalized values from the three individual donors were averaged to generate an average *Z* score and map proteins in the heatmap. *p < 0.05 (t test) and #p < 0.05 (Fisher's LSD test) compared to control.

CellPress
OPEN ACCESS

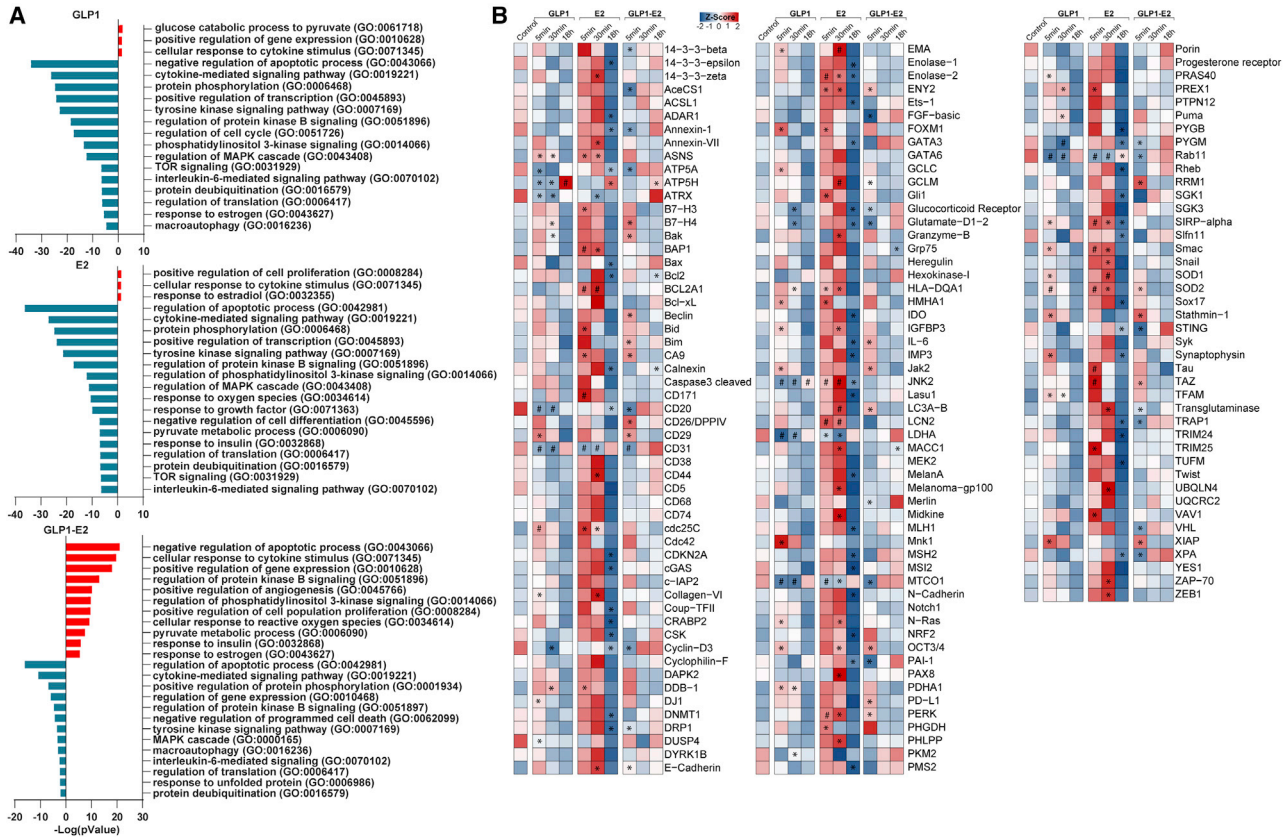

Figure 4. Effects of GLP-1, E2, and GLP1-E2 on protein expression in human islets

Cultured human islets (N = 3 donors) were treated with GLP-1, E2, or GLP1-E2 for 5 min, 30 min, and 18 h, compared to control untreated islets, and studied by RPPA.

(A) Bioinformatic analysis of major proteins pathways by GO analysis using Enrich.

(B) Heatmap of individual proteins. Normalized values from the three individual donors were averaged to generate an average *Z* score and map proteins in the heatmap; *p < 0.05 (t test) and #p < 0.05 (Fisher's LSD test) compared to control.

course of ERE activation observed in MIN6 cells treated with GLP1-E2 compared to E2 (Figures 2E and S6). In most cases, however, islets stimulated by GLP1-E2 dual agonist exhibited a protein expression pattern suggesting a combined stimulation by GLP-1 and E2 monoagonists (Figure 4B). Taken together, these results provide support for the ability of the GLP1-E2 dual agonist to recapitulate and combine the signaling generated by the monoagonists GLP-1 and E2 in cultured male human islets.

DISCUSSION

The GLP1-E2 dual agonist provides superior protection of islet β cells from metabolic stresses *in vivo* in male mouse models of diabetes compared to GLP-1 monoagonist. The doses of GLP-1 used in most animal studies to prevent diabetes are above the tolerable dose used clinically. For example, exenatide (the equivalent of the modified GLP-1 made resistant to DPP-4 used to synthesize GLP1-E2) is prescribed at a dose of 10 μg twice daily (0.12 μg/kg daily), which is a hundred times lower than the minimum dose we used, but several thousand times lower than the doses of GLP1-E2 used in previous studies (120–400 μg/kg; 30 to 100 nmol/kg).[12,14,20] That GLP1-E2 retains antidiabetic efficacy at dose ten times lower, where GLP-1 monoagonists are not efficient in mice, is consistent with the improved therapeutic index of the dual agonist over the monoagonist. The protection provided by GLP1-E2 requires GLP-1R and ERα *in vivo*, which suggests that the superior efficacy of GLP1-E2 over GLP-1 is due to E2 targeting ERα-expressing cells where GLP-1 is the potentiator and carrier to the GLP-1R-expressing target cells. We show that GLP1-E2 enters β cells through clathrin-dependent, GLP1R-mediated internalization, confirming that this larger GLP-1 conjugate is internalized like classical GLP-1 monagonists.[26,27] Notably, following GLP1-E2 internalization, E2 is activated after intracellular lysosomal acidification, likely freeing E2 to activate nuclear EREs (Figure 5). Using functional proteomics of cultured islets from male human donors, GLP1-E2 recapitulated the major signaling pathways activated by GLP-1 and E2. Ontologies used to evaluate the function of differentially expressed proteins revealed that GLP1-E2 upregulates more proteins enriched in antiapoptotic pathways, response to stress, angiogenesis, proliferation, and response to insulin, which may explain the enhanced efficacy of the dual agonist over the monoagonist. GLP1-E2-stimulated

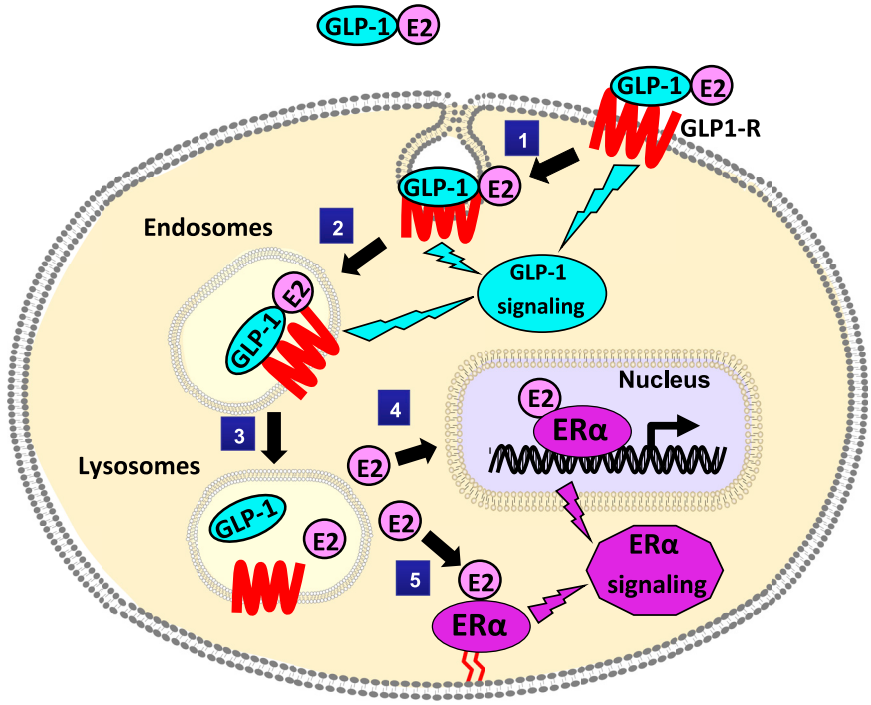

Figure 5. Summary of GLP1-E2 mechanism of action in β-cells

(1) GLP1-E2 binds GLP-1R on β cells and activates GLP-1 signaling. (2) GLP1-E2 enters β cells through clathrin-dependent, GLP1R-mediated internalization. (3) E2 is released from GLP-1 after lysosomal acidification, allowing E2 to activate nuclear and membrane-associated ERα, which promotes ERα signaling.

protein phosphorylation and expression in cultured human islets reflect peptide action in GLP-1R-expressing cells. Since islet α and β cells are the predominant cell types in human islets, while GLP-1Rs are mostly expressed in β cells,[32,33] the observed effect of GLP1-E2 likely reflects signaling in human β cells.

The GLP1-E2 dual agonist produces a delayed and prolonged E2-related proteomics signal compared with the E2 monoagonist. Similarly, compared with E2, GLP1-E2 exhibits delayed activation of nuclear EREs in MIN6 cells. This could reflect the need for intracellular processing of the GLP1-E2 conjugate prior to activate E2 action. Indeed, E2, a steroid, rapidly enters cells to activate signaling cascades in the vicinity of the plasma membrane,[34] and within 1 min of stimulation, E2 reached the nucleus of MIN6 cells to activate EREs. In contrast, GLP1-E2 must be internalized via GLP-1R (likely in endosomes), and activation of EREs from GLP1-E2 required lysosomal degradation. It is unknown whether E2 or a combination of E2 attached to a residual part of the peptide conjugate produces the estrogen output. However, it is the biological and therapeutic outcome that matters, and our data show that it can be achieved in a GLP1-E2 conjugate.

Although Sachs et al. reported that GLP1-E2 enhances glucose-stimulated insulin secretion (GSIS) in human micro-islets above that of GLP-1 and E2,[20] we found no superior insulinotropic efficacy of GLP1-E2 over the monoagonist in cultured human islets or in male wild-type mice *in vivo*.[13] Therefore, it is unlikely that GLP1-E2 prevents insulin-deficient diabetes via increased GSIS. In contrast to our *in vivo* studies, GLP1-E2 provided no additional protection of cultured mouse islets from oxidative stress-induced apoptosis compared to GLP-1 or E2 monoagonists, similar to what was reported in cultured human islets exposed to cytokine-induced apoptosis.[20] This suggests that the protection from islet destruction afforded by GLP1-E2 in mice requires additional GLP1-E2 actions in non-islet cells expressing GLP-1R and ERα, possibly in neurons or other peripheral cells involved in energy homeostasis or insulin sensitivity.[12–14] Indeed, the GLP1-E2 dual agonist improved fasting and fed glucose and insulin tolerance in wild-type mice to an extent superior to GLP1 monoagonist, independent of improvement in fat mass.[13] Additionally, GLP1-E2 may provide additional benefits from the combined GLP-1 and E2 signaling in key target cells that do not exhibit robust GLP-1R expression and are not considered classical GLP-1 targets. From that perspective, the GLP1-E2 dual agonist represents a unique pharmacological probe to identify GLP-1R and ERα co-expressing cells that are key targets of these antidiabetic actions.

In summary, GLP1-E2 enters β cells through clathrin-dependent, GLP-1R-mediated internalization, followed by E2 activation of ERs after lysosomal acidification. In human islets, GLP1-E2 recapitulates pro-survival signaling pathways activated by single agonists and mitigates insulin-deficient diabetes in male mice to a higher degree than a single GLP-1 agonist, and without feminizing effects. GLP1-E2-mediated protection of islet cells *in vivo* may require additional GLP1-E2 targeting of non-islet cells expressing GLP-1R. This study opens avenues for additional research to identify key GLP-1R and ERα co-expressing cells that mediate these antidiabetic actions. It provides support for additional studies of chemically optimized GLP1-E2 agonists with improved therapeutic index to protect functional β cell mass in situations of diabetic islet failure, like early T1D, pancreatic islet transplantation, and late stages of T2D.

Limitations of the study

Control, untreated islets, although originating from the same donors as islets treated with agonists, were not treated with vehicle for the same time courses as agonist-treated islets. However, this does not eliminate the differences in proteomics observed among the different treated conditions. Additionally, the RPPA was designed to include antibodies necessary to investigate cancer biology and lacks multiple phosphoproteins or total proteins that are key islet biology. Finally, given the heterogeneity of human islets, our small sample size (n = 3) limits the power of our analysis.

STAR★METHODS

Detailed methods are provided in the online version of this paper and include the following:

- KEY RESOURCES TABLE
- RESOURCE AVAILABILITY
  - Lead contact
  - Materials availability
  - Data and code availability
- EXPERIMENTAL MODEL AND SUBJECT DETAILS
  - Animals
  - Cell lines and cell culture
  - Human pancreatic islets
- METHOD DETAILS
  - *In vivo* studies
  - Mouse islet isolation and compounds stimulation
  - Assay for active caspase 3
  - Determination of rates of GLP1-E2 compound internalization
  - Estrogen reporter MIN6 cell line and flow cytometry
  - Reverse phase protein array (RPPA)
  - Ingenuity Pathway Analysis (IPA, Qiagen)
  - Gene ontology
  - GLP1-E2 peptides dose-response studies
  - Hormone measurements
  - Blood pressure measurement
- QUANTIFICATION AND STATISTICAL ANALYSIS

SUPPLEMENTAL INFORMATION

Supplemental information can be found online at https://doi.org/10.1016/j.xcrm.2022.100598.

ACKNOWLEDGMENTS

Human pancreatic islets were provided by the NIDDK-funded Integrated Islet Distribution Program (IIDP) (RRID:SCR _014387) at City of Hope, NIH Grant # 2UC4DK098085. This work was supported by grants from the National Institutes of Health (DK074970, DK107444), a Department of Veterans Affairs Merit Review Award (BX003725) to F.M.J, and the Tulane Center of Excellence in Sex-Based Biology & Medicine.

AUTHOR CONTRIBUTIONS

T.F. performed and analyzed experiments of ERE-GFP MIN6 cells. P.M.D.S. performed experiments of human islet culture and stimulation for RPPA and analyzed data using IPA and Enrich. M.M.F.Q. analyzed data using IPA and Enrich and generated heatmaps from RPPA. B.X., C.A., J.T., M.M., and S.H.L. performed and analyzed *in vivo* studies. B.S.Y., V.G., and R.D. synthesized, characterized, and provided GLP1-E2 compounds. F.M.J designed experiments, analyzed the data, and wrote/edited the manuscript. All the authors reviewed the manuscript.

DECLARATION OF INTERESTS

F.M.J. received consulting fees from Mithra Pharmaceutical, Inc. R.D. received research funding and is a cofounder of Marcadia biotech. R.D. has a conflict that pertains to IP at Indiana University and its license to Marcadia Biotech with Patents #9,127,088 and #9,783,592 related to this work. Other authors declare no competing financial interest.

Received: January 11, 2022
Revised: February 18, 2022
Accepted: March 15, 2022
Published: April 7, 2022

REFERENCES

1. Alonso-Magdalena, P., Ropero, A.B., Carrera, M.P., Cederroth, C.R., Baquie, M., Gauthier, B.R., Nef, S., Stefani, E., and Nadal, A. (2008). Pancreatic insulin content regulation by the estrogen receptor ER alpha. PLoS One *3*, e2069.
2. Contreras, J.L., Smyth, C.A., Bilbao, G., Young, C.J., Thompson, J.A., and Eckhoff, D.E. (2002). 17beta-Estradiol protects isolated human pancreatic islets against proinflammatory cytokine-induced cell death: molecular mechanisms and islet functionality. Transplantation *74*, 1252–1259.
3. Kilic, G., Alvarez-Mercado, A.I., Zarrouki, B., Opland, D., Liew, C.W., Alonso, L.C., Myers, M.G., Jr., Jonas, J.C., Poitout, V., Kulkarni, R.N., and Mauvais-Jarvis, F. (2014). The islet estrogen receptor-alpha is induced by hyperglycemia and protects against oxidative stress-induced insulin-deficient diabetes. PLoS One *9*, e87941.
4. Le May, C., Chu, K., Hu, M., Ortega, C.S., Simpson, E.R., Korach, K.S., Tsai, M.J., and Mauvais-Jarvis, F. (2006). Estrogens protect pancreatic beta-cells from apoptosis and prevent insulin-deficient diabetes mellitus in mice. Proc. Natl. Acad. Sci. U S A *103*, 9232–9237.
5. Liu, S., Kilic, G., Meyers, M.S., Navarro, G., Wang, Y., Oberholzer, J., and Mauvais-Jarvis, F. (2013). Oestrogens improve human pancreatic islet transplantation in a mouse model of insulin deficient diabetes. Diabetologia *56*, 370–381.
6. Liu, S., Le May, C., Wong, W.P., Ward, R.D., Clegg, D.J., Marcelli, M., Korach, K.S., and Mauvais-Jarvis, F. (2009). Importance of extranuclear estrogen receptor-alpha and membrane G protein-coupled estrogen receptor in pancreatic islet survival. Diabetes *58*, 2292–2302.
7. Tiano, J.P., Delghingaro-Augusto, V., Le May, C., Liu, S., Kaw, M.K., Khuder, S.S., Latour, M.G., Bhatt, S.A., Korach, K.S., Najjar, S.M., et al. (2011). Estrogen receptor activation reduces lipid synthesis in pancreatic islets and prevents beta cell failure in rodent models of type 2 diabetes. J. Clin. Invest. *121*, 3331–3342.
8. Tiano, J.P., and Mauvais-Jarvis, F. (2012). Importance of oestrogen receptors to preserve functional beta-cell mass in diabetes. Nat. Rev. Endocrinol. *8*, 342–351.
9. Wong, W.P., Tiano, J.P., Liu, S., Hewitt, S.C., Le May, C., Dalle, S., Katzenellenbogen, J.A., Katzenellenbogen, B.S., Korach, K.S., and Mauvais-Jarvis, F. (2010). Extranuclear estrogen receptor-alpha stimulates NeuroD1 binding to the insulin promoter and favors insulin synthesis. Proc. Natl. Acad. Sci. U S A *107*, 13057–13062.
10. Xu, B., Allard, C., Alvarez-Mercado, A.I., Fuselier, T., Kim, J.H., Coons, L.A., Hewitt, S.C., Urano, F., Korach, K.S., Levin, E.R., et al. (2018). Estrogens promote misfolded proinsulin degradation to protect insulin production and delay diabetes. Cell Rep. *24*, 181–196.
11. Mauvais-Jarvis, F., Clegg, D.J., and Hevener, A.L. (2013). The role of estrogens in control of energy balance and glucose homeostasis. Endocr. Rev. *34*, 309–338.
12. Finan, B., Yang, B., Ottaway, N., Stemmer, K., Muller, T.D., Yi, C.X., Habegger, K., Schriever, S.C., Garcia-Caceres, C., Kabra, D.G., et al. (2012). Targeted estrogen delivery reverses the metabolic syndrome. Nat. Med. *18*, 1847–1856.
13. Tiano, J.P., Tate, C.R., Yang, B.S., DiMarchi, R., and Mauvais-Jarvis, F. (2015). Effect of targeted estrogen delivery using glucagon-like peptide-1 on insulin secretion, insulin sensitivity and glucose homeostasis. Sci. Rep. *5*, 10211.
14. Schwenk, R.W., Baumeier, C., Finan, B., Kluth, O., Brauer, C., Joost, H.G., DiMarchi, R.D., Tschop, M.H., and Schurmann, A. (2014). GLP-1-oestrogen attenuates hyperphagia and protects from beta cell failure in diabetes-prone New Zealand obese (NZO) mice. Diabetologia *58*, 604–614.

15. Hatamori, N., Yokono, K., Hayakawa, M., Taki, T., Ogawa, W., Nagata, M., Hari, J., Shii, K., Taniguchi, H., and Baba, S. (1990). Anti-interleukin 2 receptor antibody attenuates low-dose streptozotocin-induced diabetes in mice. Diabetologia *33*, 266–271.

16. Ihm, S.H., Lee, K.U., Rhee, B.D., and Min, H.K. (1990). Initial role of macrophage in the development of anti-beta-cell cellular autoimmunity in multiple low-dose streptozotocin-induced diabetes in mice. Diabetes Res. Clin. Pract. *10*, 123–126.

17. Kantwerk-Funke, G., Burkart, V., and Kolb, H. (1991). Low dose streptozotocin causes stimulation of the immune system and of anti-islet cytotoxicity in mice. Clin. Exp. Immunol. *86*, 266–270.

18. Lukic, M.L., Stosic-Grujicic, S., and Shahin, A. (1998). Effector mechanisms in low-dose streptozotocin-induced diabetes. Dev. Immunol. *6*, 119–128.

19. McEvoy, R.C., Thomas, N.M., Hellerstrom, C., Ginsberg-Fellner, F., and Moran, T.M. (1987). Multiple low-dose streptozotocin-induced diabetes in the mouse: further evidence for involvement of an anti-B cell cytotoxic cellular auto-immune response. Diabetologia *30*, 232–238.

20. Sachs, S., Bastidas-Ponce, A., Tritschler, S., Bakhti, M., Böttcher, A., Sánchez-Garrido, M.A., Tarquis-Medina, M., Kleinert, M., Fischer, K., Jall, S., et al. (2020). Targeted pharmacological therapy restores β-cell function for diabetes remission. Nat. Metab. *2*, 192–209.

21. Dejgaard, T.F., Frandsen, C.S., Hansen, T.S., Almdal, T., Urhammer, S., Pedersen-Bjergaard, U., Jensen, T., Jensen, A.K., Holst, J.J., Tarnow, L., et al. (2016). Efficacy and safety of liraglutide for overweight adult patients with type 1 diabetes and insufficient glycaemic control (Lira-1): a randomised, double-blind, placebo-controlled trial. Lancet Diabetes Endocrinol. *4*, 221–232.

22. Frandsen, C.S., Dejgaard, T.F., Holst, J.J., Andersen, H.U., Thorsteinsson, B., and Madsbad, S. (2015). Twelve-week treatment with liraglutide as add-on to insulin in normal-weight patients with poorly controlled type 1 diabetes: a randomized, placebo-controlled, double-blind parallel study. Diabetes Care *38*, 2250–2257.

23. Bettge, K., Kahle, M., Abd El Aziz, M.S., Meier, J.J., and Nauck, M.A. (2017). Occurrence of nausea, vomiting and diarrhoea reported as adverse events in clinical trials studying glucagon-like peptide-1 receptor agonists: a systematic analysis of published clinical trials. Diabetes Obes. Metab. *19*, 336–347.

24. Liu, M., Hodish, I., Haataja, L., Lara-Lemus, R., Rajpal, G., Wright, J., and Arvan, P. (2010). Proinsulin misfolding and diabetes: mutant INS gene-induced diabetes of youth. Trends Endocrinol. Metab. *21*, 652–659.

25. Goke, R., Fehmann, H.C., Linn, T., Schmidt, H., Krause, M., Eng, J., and Goke, B. (1993). Exendin-4 is a high potency agonist and truncated exendin-(9-39)-amide an antagonist at the glucagon-like peptide 1-(7-36)-amide receptor of insulin-secreting beta-cells. J. Biol. Chem. *268*, 19650–19655.

26. Jones, B., Buenaventura, T., Kanda, N., Chabosseau, P., Owen, B.M., Scott, R., Goldin, R., Angkathunyakul, N., Corrêa, I.R., Jr., Bosco, D., et al. (2018). Targeting GLP-1 receptor trafficking to improve agonist efficacy. Nat. Commun. *9*, 1602.

27. Buenaventura, T., Bitsi, S., Laughlin, W.E., Burgoyne, T., Lyu, Z., Oqua, A.I., Norman, H., McGlone, E.R., Klymchenko, A.S., Corrêa, I.R., Jr., et al. (2019). Agonist-induced membrane nanodomain clustering drives GLP-1 receptor responses in pancreatic beta cells. PLoS Biol. *17*, e3000097.

28. Dutta, D., Williamson, C.D., Cole, N.B., and Donaldson, J.G. (2012). Pitstop 2 is a potent inhibitor of clathrin-independent endocytosis. PLoS One *7*, e45799.

29. Sloop, K.W., Willard, F.S., Brenner, M.B., Ficorilli, J., Valasek, K., Showalter, A.D., Farb, T.B., Cao, J.X., Cox, A.L., Michael, M.D., et al. (2010). Novel small molecule glucagon-like peptide-1 receptor agonist stimulates insulin secretion in rodents and from human islets. Diabetes *59*, 3099–3107.

30. Willard, F.S., Ho, J.D., and Sloop, K.W. (2020). Discovery and pharmacology of the covalent GLP-1 receptor (GLP-1R) allosteric modulator BETP: a novel tool to probe GLP-1R pharmacology. Adv. Pharmacol. *88*, 173–191.

31. Yoshimori, T., Yamamoto, A., Moriyama, Y., Futai, M., and Tashiro, Y. (1991). Bafilomycin A1, a specific inhibitor of vacuolar-type H(+)-ATPase, inhibits acidification and protein degradation in lysosomes of cultured cells. J. Biol. Chem. *266*, 17707–17712.

32. McLean, B.A., Wong, C.K., Campbell, J.E., Hodson, D.J., Trapp, S., and Drucker, D.J. (2021). Revisiting the complexity of GLP-1 action from sites of synthesis to receptor activation. Endocr. Rev. *42*, 101–132.

33. Ast, J., Arvaniti, A., Fine, N.H.F., Nasteska, D., Ashford, F.B., Stamataki, Z., Koszegi, Z., Bacon, A., Jones, B.J., Lucey, M.A., et al. (2020). Super-resolution microscopy compatible fluorescent probes reveal endogenous glucagon-like peptide-1 receptor distribution and dynamics. Nat. Commun. *11*, 467.

34. Mauvais-Jarvis, F., Lange, C.A., and Levin, E.R. (2021). Membrane-initiated estrogen, androgen and progesterone receptor signaling in health and disease. Endocr. Rev., bnab041. https://doi.org/10.1210/endrev/bnab041.

35. Hewitt, S.C., Kissling, G.E., Fieselman, K.E., Jayes, F.L., Gerrish, K.E., and Korach, K.S. (2010). Biological and biochemical consequences of global deletion of exon 3 from the ER alpha gene. FASEB J. *24*, 4660–4667.

36. Smith, E.P., An, Z., Wagner, C., Lewis, A.G., Cohen, E.B., Li, B., Mahbod, P., Sandoval, D., Perez-Tilve, D., Tamarina, N., et al. (2014). The role of β cell glucagon-like peptide-1 signaling in glucose regulation and response to diabetes drugs. Cell Metab. *19*, 1050–1057.

STAR★METHODS

KEY RESOURCES TABLE

REAGENT or RESOURCE	SOURCE	IDENTIFIER
Antibodies		
RPPA antibodies	MD-Anderson Cancer Center	https://www.mdanderson.org/research/research-resources/core-facilities/functional-proteomics-rppa-core/antibody-information-and-protocols.html
Biological samples		
De-identified human pancreatic islets	PRODO Laboratories Inc	https://prodolabs.com/
Chemicals, peptides, and recombinant proteins		
GLP1	Richard D. DiMarchi	N/A
GLP1-E2	Richard D. DiMarchi	N/A
iGLP1-E2	Richard D. DiMarchi	N/A
GLP1-E2-Rho, red	Richard D. DiMarchi	N/A
17β-Estradiol (E2)	Steraloids	Cat# E0950-000
Exendin 9-39	Sigma Aldrich	Cat# E7269
Streptozotocin	Sigma Aldrich	Cat# 18883-66-4
D-(+)-Glucose	Sigma Aldrich	Cat# G7528
PBS	Gibco	Cat# 10010023
HBSS	Gibco	Cat# 14025092
Phenol-red free RPMI-1640 medium	Gibco	Cat# 11835030
DMEN medium	Gibco	Cat# 11965126
Phenol-red free DMEN medium	Gibco	Cat# 21063029
HEPES	Gibco	Cat# 15630080
Sodium Pyruvate	Gibco	Cat# 11360070
GlutaMAX	Gibco	Cat# 35050061
Penicillin/streptomycin	Gibco	Cat# 15140063
Collagenase	Sigma Aldrich	Cat# C9263
Charcoal Stripped FBS	GemCell™	Cat# 100-119
FBS	GemCell™	Cat# 100-500
Ethanol	Sigma Aldrich	Cat# E7023
H_2O_2	Sigma Aldrich	Cat# 216763
AF488-Dex	ThermoFisher	Cat# D22910
Pitstop-2	Sigma Aldrich	Cat# SML1169
Puromycin	ThermoFisher	Cat# A1113802
Critical commercial assays		
Caspase-Glo 3/7 assay kit	Promega	Cat# G8090
TRUEresult glucose meter	Nipro Diagnostics	Cat# E4NPD03
Rat/Mouse Insulin ELISA kit	Millipore	Cat# EZRMI-13K
Testosterone Elisa	IBL America	Cat# IB79106
Luteinizing hormone Elisa	LSBio	Cat# LS-F22503-1
17β-estradiol Elisa	Calbiotech	Cat# ES380S
Experimental models: Cell lines		
MIN6 cells	Dr. Koizumi Laboratory	N/A
Experimental models: Organisms/strains		
Mouse: C57BL/6J	The Jackson Laboratory	Strain #000664
Mouse: C57BL/6-Ins2Akita/J	The Jackson Laboratory	Strain #003548

(*Continued on next page*)

Continued		
REAGENT or RESOURCE	SOURCE	IDENTIFIER
Mouse: Esr1$^{fl/fl}$	Dr. Kenneth Korach	N/A
Mouse: Sox2-cre$^{Tg(Sox2\text{-}cre)1Amc}$/J	The Jackson Laboratory	Strain #008454
Mouse: Glp1r$^{f/f}$	Dr. David D'Alessio	N/A
Mouse: Ins2-cre$^{Tg(Ins2\text{-}cre)25Mgn}$/J	The Jackson Laboratory	Strain # 003573
Recombinant DNA		
ER-RE-GFP lentivirus	GenTarget Inc	Cat# LVP973-P
Software and algorithms		
Gen5 imager software	Agilent	https://www.biotek.com/products/software-robotics-software/gen5-microplate-reader-and-imager-software/
Elements Advanced Research software	Nikon	https://www.microscope.healthcare.nikon.com/products/software/nis-elements/nis-elements-advanced-research
RStudio v1.2.1335 (64x bit, for Windows)	The R Consortium	https://www.rstudio.com/products/
Ingenuity Pathway Analysis (IPA)	Qiagen	https://digitalinsights.qiagen.com/products-overview/discovery-insights-portfolio/analysis-and-visualization/qiagen-ipa/?cmpid=QDI_GA_IPA&gclid=Cj0KCQiA3rKQBhCNARIsACUEW_beTxh0IgfRAtfWcvbawY1cFpVLowb2G6pe8Qf7jWZtJY1s6KfuAGIaAuxEEALw_wcB
GraphPad Prism v8	GraphPad	https://www.graphpad.com/
Kaluza v1.5a and v2.1.1	Beckman Coulter	https://www.beckman.com/flow-cytometry/software/kaluza
CODA® High Throughput System	Kent Scientific Corporation	https://www.kentscientific.com/products/coda-high-throughput-system/
EnrichR	Developed in the Ma'ayan Lab	https://maayanlab.cloud/Enrichr/

RESOURCE AVAILABILITY

Lead contact

Further information and requests for resources and reagents should be directed to and will be fulfilled by the lead contact, Franck Mauvais-Jarvis (fmauvais@tulane.edu).

Materials availability

This study did not generate any new materials.

Data and code availability

- All data reported in this paper will be shared by the Lead contact upon request.
- A description of coding environments required to reproduce the heatmaps in this paper are outlined in: https://github.com/fmjlab/GLP1-E2-Manuscript.
- Any additional information required to reanalyze the data reported in this paper is available from the Lead contact upon request.

EXPERIMENTAL MODEL AND SUBJECT DETAILS

Animals

Eight- to ten-week-old male wild type mice (C57BL/6J, The Jackson Laboratory) were used for MLD-STZ induction of diabetes and caspase 3 assays. Three- to six-week-old Akita male mice (C57BL/6-Ins2^{Akita}/J) were used as a model of type 1 diabetes (The Jackson Laboratory). ERαKO mice were kindly provided by Dr. Kenneth Korach (NIEHS).[35] Esr1fl/fl mice were generated by flanking exon 3 of Esr1 gene by loxP sites. The construct was electroporated into C57BL/6N Tac ES cells, which were then injected into B6 albino blastocysts. Resulting chimeras were then bred with B6 albino females and black F1 pups were genotyped for the presence of the floxed allele (Caliper Life Sciences, Cranbury, NJ, USA). The Esr1 was deleted globally by crossing mice carrying floxed exon 3 Esr1 with a global Sox2-cre (Tg(Sox2-cre)1Amc/J; Jackson Laboratories, Bar Harbor ME, USA), which expresses Cre activity in the epiblast line

allowing germ-line deletion of targeted genes. Glp1r$^{f/f}$ mice were kindly provided by Dr. David D'Alessio (Duke University). Briefly, Glp1r gene was target by vector containing neomycin (NEO) resistance selection cassette flanked by flippase (FLP) recognition target (FRT) sites, and loxP sites on either side exons 6 and 7 of the Glp1r gene.[36] Glp1r was deleted from pancreatic β-cells by crossing *Glp1r*$^{f/f}$ mice with RIP-cre (Tg(Ins2-cre)25Mgn/J; Jackson Laboratories, Bar Harbor ME, USA). All mice used in our studies were housed with free access to food and water with a 14:10 light:dark cycle. Experiments were approved by the Tulane University Institutional Animal Care and Use Committee and conducted in accordance with the National Institutes of Health guidelines.

Cell lines and cell culture

Mouse Insulinoma 6 (MIN6) cells were obtained from Dr. Koizumi Laboratory at Kyoto University and cultured at 37°C in DMEM medium (Gibco, 11965126) with 10% fetal bovine serum (GemCell™, 100-500) and Penicillin-Streptomycin (Gibco, 15140063). Drugs used in culture studies were glucagon-like peptide-1 (GLP1, 10^{-8}M), GLP-1 covalently fused to E2 (GLP1-E2, 10^{-8}M) and an inactive GLP-1 covalently fused to E2 (iGLP1-E2, 10^{-8}M). The synthesis of GLP-E2 conjugates has been previously described.[12] For each compound, the *in vivo* dose of 120 μg/kg is equivalent to the *in vitro* dose of 10^{-8}M.[12]

Human pancreatic islets

De-identified human pancreatic islets from three male donors were obtained from PRODO Laboratories Inc. Donors information: 37 year old African American, BMI of 28.0; 67 year old Asian, BMI of 24.4 and 55 year old Caucasian, BMI of 25.6. Islets were left in culture at 37°C overnight before any experiments were performed. Islets were cultured in phenol-red free RPMI medium (Gibco, 11835030) containing 11mM glucose, supplemented with 10% Charcoal Stripped FBS, HEPES (Gibco, 15630080), Sodium Pyruvate (Gibco, 11360070), GlutaMAX (Gibco, 35050061) and Penicillin-Streptomycin (Gibco, 15140063).

METHOD DETAILS

In vivo studies

Male Akita mice were treated daily with intraperitoneal (i.p.) injection of 120 μg/kg/day GLP1, GLP1-E2, exendin 9-39 (Sigma-Aldrich, E7269) or vehicle PBS (Gibco, 10010023). For induction of diabetes C57BL/6J mice were injected (i.p) 50 mg/kg streptozotocin (Sigma-Aldrich, 18883-66-4) for five days following 10 hours fast prior to each injection. Random fed blood glucose was measured by tail bleeding. For GTT, mice were fasted overnight for 15 hours prior to i.p. injection of (2g/kg) glucose (Sigma Aldrich, G7528). Blood glucose concentrations were measured using a TRUEresult glucose meter (Nipro Diagnostics, E4NPD03). Plasma insulin levels were quantified using the Rat/Mouse Insulin ELISA kit (Millipore, EZRMI-13K).

Mouse islet isolation and compounds stimulation

Mouse islet isolation was performed as described.[7] Briefly, the common bile duct was cannulated, and the pancreas was perfused with solution of HBSS (Gibco, 14025092) containing 1.5 mg/mL collagenase (Sigma-Aldrich, C9263). Pancreas was excised, digested for 10 minutes and rinsed with ice-cold HBSS. Islets were hand-picked under a dissection microscope and transferred into a dish filled with phenol-red free RPMI-1640 medium (Gibco, 11835030) supplemented with 10% CS-FBS (GemCell™, 100-119). Islets were incubated with 10^{-8}M E2 (Steraloids Inc, E0950-000), GLP-1 (10^{-8}M) and GLP1-E2 (10^{-8}M) for 48h. Ethanol was used as the vehicle. Following 48h ER ligand treatment, islets were exposed to 100 μM H_2O_2 (Sigma-Aldrich, 216763) for the last 5 hours, prior to assessment of apoptosis.

Assay for active caspase 3

Caspase activity was measured in mouse islets using Caspase-Glo 3/7 assay kit (Promega, G8090). Briefly, after 5h incubation with 100μM H_2O_2 (Sigma-Aldrich, 216763), islets were centrifuged for 5 min at 1200 rpm and transferred to a 96-well plate in 100 μL medium. Islets were then lysed with 100 μL Caspase-Glo 3/7 reagent and incubated at room temperature for 30min. Luciferase activity was measured using a *Synergy*™ *2* Multi-Mode Microplate Reader *(*BioTek). Values are reported as relative luciferase units corrected for total protein concentration.

Determination of rates of GLP1-E2 compound internalization

MIN6 cells were cultured on a microscope cover 8-chamber slide in 10% FBS (GemCell™,100-500) DMEM media (Gibco, 11965126) for 2 days prior to experiment. On the day of the experiment, cells were mounted into the Tokai Hit live cell incubator chamber and washed with serum-free phenol-free DMEM (Gibco, 21063029) followed by addition of DMEM containing a 0.015mg/mL AF488-Dex (ThermoFisher, D22910) to find the optimal confocal plane prior to peptide addition. Where applicable, 25μM Pitstop-2 (Sigma Aldrich, SML1169) was added to cells 10 minutes prior to peptide addition. Once an optimal confocal plane was established, DMEM containing AF488–Dex (and Pitstop-2) was removed and replaced with DMEM containing 0.015mg/mL AF488-Dex and 2μM rhodamine-labeled peptide. Confocal images were captured over 15 minutes on a Nikon A-1 at intervals of 30 seconds, which resulted in 30 images per treatment. Laser scans used to excite fluorescent reagents were performed sequentially to avoid bleed-over. Rates of internalization were calculated using Nikon Elements Advanced Research software. A region of interest containing several adjacent cells (object area) was selected by the software for each frame from the rhodamine channel. A threshold for absence

of pixel density was assigned at time 0 and measured as percentage of object area. Loss of object area (internalization of rhodamine signal) between 0 and 15 min occurred if the software detected increased pixel density within the region of interest because of rhodamine signal entering the cell. The percentage of object area (internalization) was calculated for each frame (time point) and then plotted as a loss of object area over time. One-phase decay kinetics were used to calculate a rate from the percentage of object area loss over time and presented as rates of internalization.

Estrogen reporter MIN6 cell line and flow cytometry

MIN6 cells were stably transduced using a lentivirus delivering a 4 tandem ER-RE-driven GFP (ERE-GFP) (Gentarget Inc, LVP973-P) according to the manufacturer's instructions. Puromycin (ThermoFisher, A1113802) (2μg/mL) was used to select stably transduced ERE-GFP MIN6 cells. Before performing an experiment, ERE-GFP MIN6 cells were cultured in phenol-free DMEM media containing 10% charcoal-stripped FBS for 7 days and for the duration of the experiment. GFP fluorescence was measured in ERE-GFP MIN6 cells treated with compounds the next day using flow cytometry. Vehicle treated ERE-GFP MIN6 cells were used to establish gating to quantify the percentage of GFP positivity in ERE-GFP MIN6 cells treated with compounds.

Reverse phase protein array (RPPA)

Human islets from male human donors (N = 3 donors) were obtained from PRODO Laboratories Inc and were cultured overnight and treated with E2 (Steraloids, E0950-000), GLP1 or GLP1-E2 (10^{-8} M) for 5 minutes, 30 minutes or for 18 hours. Control islets received no treatment. Islets were stored at −80°C until shipment to MD Anderson Cancer Center Functional Proteomics RPPA Core Facility. Cell lysates were serially diluted twofold for 5 dilutions (undiluted, 1:2, 1:4, 1:8; 1:16) and arrayed on nitrocellulose-coated slides in an 11x11 format to produce sample spots. Sample spots were then probed with 485 unique antibodies by a tyramide-based signal amplification approach and visualized by DAB colorimetric reaction to produce stained slides. Stained slides were scanned on a Huron TissueScope scanner to produce 16-bit tiff images. Sample spots in tiff images were identified and their densities quantified by Array-Pro Analyzer. Relative protein levels for each sample were determined by interpolating each dilution curve produced from the densities of the 5-dilution sample spots using a "standard curve" (SuperCurve) for each slide (antibody). All relative protein level data points were normalized for protein loading and transformed to linear values. Protein levels were further normalized by GAPDH and β-actin. Enrichment (fold-change) between treatment and control groups were reported for all phospho and total proteins of interest. For heatmap representation, proteins were normalized via a Z-test in R using customized scripts and plotted using the ggplot2 and heatmap.2 packages.

Ingenuity Pathway Analysis (IPA, Qiagen)

The IPA Downstream Effects Analysis algorithm was used to identify biological functions that were expected to increase or decrease, given the observed phosphorylation changes of our dataset. Downstream Effects Analysis is based on expected causal effects between phosphoproteins and functions; the expected causal effects are derived from the literature compiled in the QIAGEN Knowledge Base. The analysis examined phosphoproteins that are known to affect diseases and functions, compared the phosphoproteins direction of change to expectations derived from the literature, then issued a prediction for each biological function based on the direction of change. The direction of change is the phosphorylation in the experimental samples relative to the control group. If the direction of change is: 1) consistent with the literature across most phosphoproteins, IPA predicted that the biological function increases in the experimental sample; 2) inconsistent with the literature, IPA predicted that the biological function decreases; 3) shows no clear pattern related to the literature, IPA did not make a prediction. IPA used the z-score algorithm to make predictions. The z-score algorithm is designed to reduce the chance that random data will generate significant predictions.

Gene ontology

The gene ontology (GO) enrichment analysis included proteins expression at 18h into the treatments. Proteins were analyzed using Enrichr (https://maayanlab.cloud/Enrichr/), focusing on the "Biological Process" domain, and considered the main annotations that were up- or downregulated by the three compounds with an adjusted p-value < 0.01. Heatmaps were generated for normalized protein expression in R v4.0.2 using the heatmap.2 package.

GLP1-E2 peptides dose-response studies

The GLP-1 activities of the GLP-1, GLP1-E2 and iGLP1-E2 conjugates were tested by the measurements of cAMP production on GLP-1 receptor expressing and luciferase reporter assay gene engineering cells described previously.[12]

Hormone measurements

Blood was sampled for measurement of testosterone (IBL America, IB79106), luteinizing hormone (LSBio, LS-F22503-1), and 17β-estradiol (Calbiotech, ES380S) by ELISA.

Blood pressure measurement

Conscious blood pressure was measured using tail-cuff plethysmography (CODA system, Kent Scientific) while warming at 35°C under slight restraint. Eight to ten weeks C57BL/6J male mice were acclimated to the restraint tube and then subjected to three days of

baseline measurements. Each session included 10-15 readings for each mouse, and readings that lacked a significant increase in flow during deflation were excluded. Baseline measurements were the average of three sessions. On the day of testing, blood pressure was recorded two hours after injection of vehicle, GLP-1 or GLP1-E2.

QUANTIFICATION AND STATISTICAL ANALYSIS

Results were presented as means ± SEM and analyzed by Student's t-test or one-way ANOVA followed by a post-hoc Bonferroni test or Fisher's LSD test when appropriate with Graphpad Prism 9 software. $p < 0.05$ was considered as statistically significant.